



**Acoustics'08  
Paris**  
June 29-July 4, 2008

[www.acoustics08-paris.org](http://www.acoustics08-paris.org)

## Ultraviolet detector based on a surface acoustic wave oscillator system with ZnO-nanostructure sensing material

Tsung-Tsong Wu<sup>a</sup>, Wei-Shan Wang<sup>a</sup>, Tai-Hsu Chou<sup>a</sup> and Yung-Yu Chen<sup>b</sup>

<sup>a</sup>Institute of Applied Mechanics, National Taiwan University, No. 1, Sec. 4, Roosevelt Road, 106 Taipei, Taiwan

<sup>b</sup>Department of Mechanical Engineering, Tatung University, No. 40, Sec. 3, Chungshan N. Rd., 104 Taipei, Taiwan  
dainty@ndt.iam.ntu.edu.tw

Recently, ultraviolet (UV) detectors based on surface acoustic wave (SAW) devices utilizing the acoustoelectric effect have been demonstrated. However, most of presented cases were based on semiconductor sensing films. In this paper, ZnO-nanostructure and a dual delay line SAW oscillator system are combined to develop a high precision UV detector. The UV detector is made of ZnO nanorod on a 128°YX-LiNbO<sub>3</sub>-based SAW device. The operating frequency is at 145MHz. The system is illuminated by a UV source consists of a Xe lamp and a monochromator, resulting in frequency shifts. Under illumination of 365, 370 and 375nm for several on-off cycles, a maximum value of over 40 kHz are observed at 365nm, indicating the ZnO nanorod-based detector is most sensitive to 365nm-UV light and with good repeatability. Moreover, frequency shifts reach a value of 19 kHz in 10 seconds after 365nm is on, which implies this is a real-time high-sensitivity UV sensor. These results show the ZnO-nanostructure based SAW oscillator is a promising candidate for a real-time, fast-response, high-precision UV detector.

## 1 Introduction

One-dimensional ZnO film, a well-known semiconducting and piezoelectric material, has been widely used in electronic applications. ZnO is also sensitive to ultraviolet due to its attractive optical properties, including wide band-gap of 3.4eV and large exciton binding energy of 60 meV at room temperature. Large photoresponse of ZnO thin film makes it be a promising material used in optical and optoelectric applications.

Recently, there has been a growing interest in investigating the properties of nanostructured ZnO. A number of studies focused on the synthesis of ZnO nanostructures such as nanowires [1], nanorods [2] and nanobelts [3] have been reported. Researches on ZnO nanostructures also have drawn much attention because of their excellent physical properties as well as ZnO film. Moreover, ZnO nanostructures have large surface-to-volume ratio, deep penetration depth and fast charge diffusion rate. Thus, ZnO nanostructure with favorable properties as described can be demonstrated as a candidate material for broad applications in technology, including UV lasers [4], field emitters [5] and solar cells [6]. Furthermore, due to properties including high sensitivity, rapid response, and fast recovery, ZnO nanostructure are also widely used as sensing materials in humidity sensors [7], gas sensors [8], and biosensors [9].

Surface acoustic wave devices have been in commercial use for over decades. SAW RF (radio frequency) and IF (intermediate frequency) filters of the transceiver electronics are widely used in telecommunications industry because of their small size, low cost, and high performance. Besides, there are growing interests on SAW sensors for which most energy is confined within one wavelength of the surface, leading to high sensitivity. In addition, SAW sensors are passive, stable, and can be applied for wireless remote sensing and control. Therefore, SAW sensors are promising candidates for a variety of sensors such as gas [10], humidity [11], pressure [12], and biosensors [13]. Several SAW-based UV detectors utilizing the acoustoelectric effect have been demonstrated [14-16]. However, most of presented cases were based on semiconductor sensing films.

In the present paper, a ZnO-nanorod and a dual delay line SAW oscillator system are combined to develop a high precision UV detector. The frequency shifts related to different optical wavelengths and power density will be measured and discussed in the following sections.

## 2 Sensor design and fabrication

### 2.1 Design and fabrication of a two-port SAW resonator

The change in SAW velocity due to acoustoelectric interaction is proportional to the electromechanical coupling coefficient  $K^2$  [17]. A material with a large coupling coefficient such as LiNbO<sub>3</sub> is highly suitable for UV detecting utilizing acoustoelectric effect. High piezoelectricity of LiNbO<sub>3</sub> not only offers excellent piezoelectric conversion but also scales down the size of a SAW device by reducing IDT pairs. Therefore, we fabricate SAW oscillators on a 128°YX-LiNbO<sub>3</sub> substrate. The designed center frequency of the two-port SAW resonator is 145MHz. The design parameters of IDT are listed in Table 1. A 150nm-thick aluminum film was deposited on 128°YX-LiNbO<sub>3</sub> by sputtering, followed by lithography and etching process, to form the electrodes. Frequency responses of the fabricated SAW devices were then measured by a network analyzer, the center frequencies are all around 145.87MHz and insertion losses are in a range from -5 to -7dB. Measurement results show the performance of these SAW devices is quite well.

Wavelength	27 $\mu$ m
Finger space	6.75 $\mu$ m
Aperture	2700 $\mu$ m
Delay line	4320 $\mu$ m
IDT pairs	15
No. of reflectors	50

Table 1 IDT design parameters

### 2.2 ZnO nanorod growth

In this study, chemical solution method [18] is adopted for ZnO nanorods growth. First, a 50 nm-thick ZnO film used as a seed layer was deposited on a fabricated SAW device by sputtering. It should be noticed that ZnO films and the

followed nanorods were grown only on the delay line between two IDT electrodes, namely, the sensing area. Then the seeded LiNbO<sub>3</sub> substrate was immersed in a solution containing a mixture of zinc nitrate hydrate (0.025 M) and methenamine (0.025 M) at 95 °C for 6 h. After this treatment, the substrate was rinsed with deionized water and dried by Nitrogen gas. Fig. 1 is a SEM image of a top view of the ZnO nanorods. Average diameter of the ZnO nanorods is less than 150nm. Height of the ZnO nanorods is about 450nm.

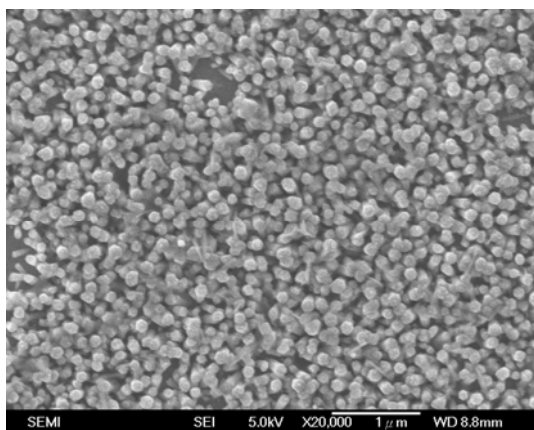


Fig.1 A SEM Image of ZnO Nanorods.

### 2.3 Construction of the sensing system

In order to eliminate environment fluctuations such as temperature and pressure, stability of a SAW sensor is needed to optimize the performance of the SAW sensor. These fluctuations can be ruled out by using a dual delay line SAW oscillator. In this study, a dual channel SAW oscillator consists of two counterparts, one is a SAW device coated with a ZnO-nanorod sensing material and the other one remains the bare surface, is constructed. Fig. 2 shows that the oscillators were connected to amplifiers, a mixer, and a low pass filter to form a dual delay line SAW oscillator system.

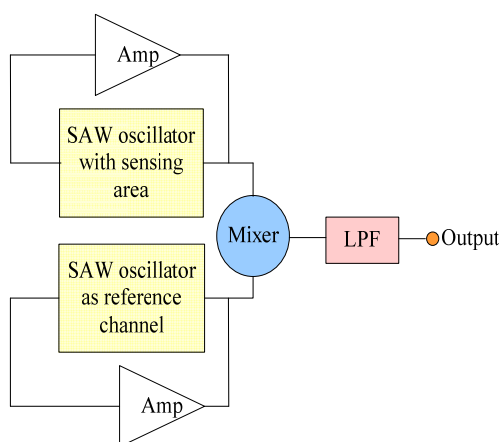


Fig.2 Illustration of the Dual Channel Configuration.

The experimental setup of a UV detecting system is shown in Fig 3. The sensing area of the dual delay line SAW oscillator was illuminated by a UV source consists of a Xe

lamp and a monochromator. When the ZnO nanorod sensing area was subjected to UV illumination, a frequency shift was observed. The frequency differences were fed to a frequency counter connected with a personal computer for real-time data acquisition and storing.

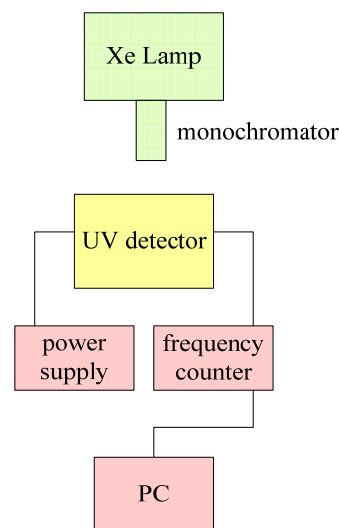


Fig.3 Experimental Setup of a UV Detecting System

## 3 Measurement results

Before a UV source is switched on, there exists a basic frequency difference between the reference channel and the sensing channel, which oscillates about 1.3MHz, as shown in Fig. 4. All measurements described next will be done after the SAW UV sensor has reached a steady state with low noise. First, we will discuss the response and repeatability of the UV detector by varying the wavelength of the UV source. By proper adjusting the distance between the sensor and light source, the power of the UV source can be set constant to 3.5mW/cm<sup>2</sup> even when the wavelengths are changed. The UV detector was under UV irradiation with three UV lights, 365nm, 370nm, and 375nm, respectively. In Fig.4, the arrows represent that UV irradiation is on, and the triangles represent that UV source is off. Frequency shifts were immediately measured when the device was under 365nm irradiation toward 3 on-off cycles, 370nm for 2 cycles, and 375nm for 2 cycles subsequently. It should be noticed that when the sensor is illuminated by UV light for the first time, there would be a frequency shift due to dark conductivity, resulting in larger shift corresponding to the following measurement, as the position of the first arrow shown in Fig. 4. It shows that the maximum frequency shift occurs at the optical wavelength of 365nm, and gradually decreased as the wavelengths become larger, indicating that the acoustoelectric interaction is most effective when the optical wavelength is 365nm, resulting the UV sensor be most sensitive at 365nm.

Fig. 5 shows the response of the UV detector under 650nm illumination. The optical wavelength at 650nm is turned on at 10 sec and turned off at 120sec. It shows that the UV detector is insensitive to a wavelength outside the UV range. Maximum frequency shift is about 3 kHz, corresponding to the noise level when the sensor oscillates at a steady state

without UV illumination. In addition, even when the light power at 650nm becomes larger, the UV detector remains insensitive. Therefore, a UV detector based on dual-channel SAW oscillator system with ZnO-nanorod sensing area can achieve goals such as eliminating environmental fluctuations and also being insensitive to other optical wavelengths out of the UV range.

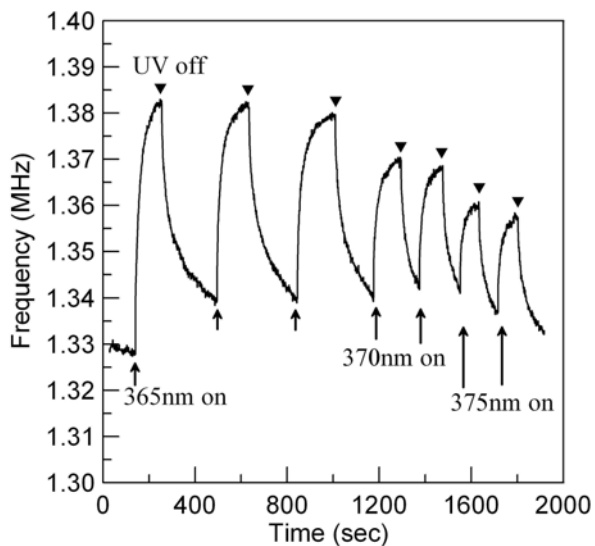


Fig.4 Sensing Response of the UV Detector with Different Light Wavelengths

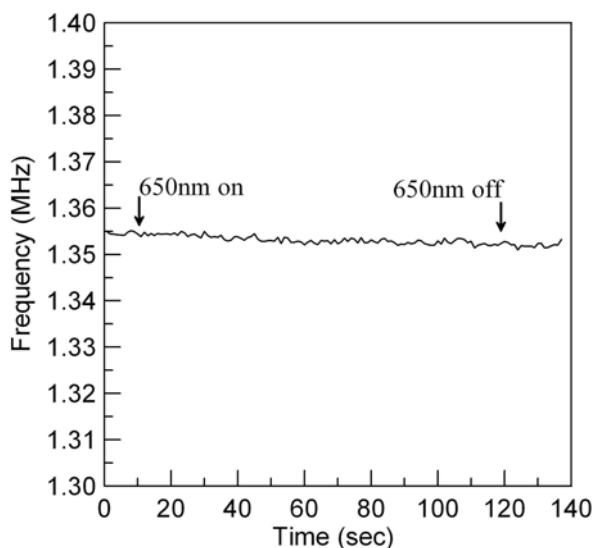


Fig.5 Sensing Response of the UV Detector under 650nm Illumination

As mentioned before, the ultraviolet detector has largest response at 365nm. Thus the UV source is chosen as 365nm for following discussion on detector response toward different light power. Frequency shifts of UV on-off cycle for three times were recorded at different power densities. The experimental data is illustrated in Fig. 6. As can be seen, maximum frequency shifts are 44 kHz, 26 kHz, and 12 kHz corresponding to 3.5mW/cm<sup>2</sup>, 1.6mW/cm<sup>2</sup>, and 0.5mW/cm<sup>2</sup>. Average frequency shifts of these measurements are 42 kHz at 3.5mW/cm<sup>2</sup>, 24 kHz at 1.6mW/cm<sup>2</sup> and 12 kHz at 0.5mW/cm<sup>2</sup>, respectively.

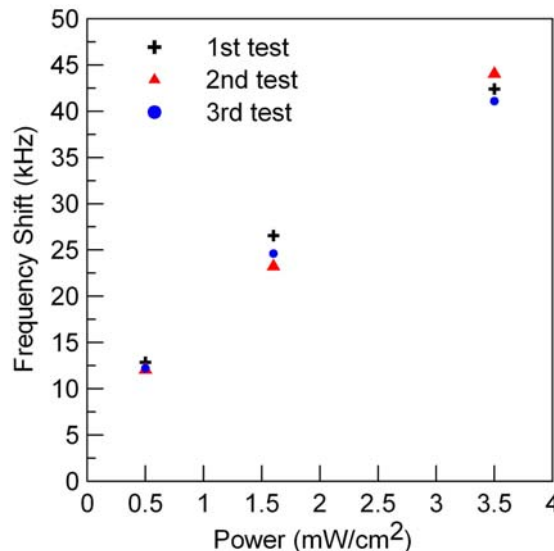


Fig.6 Frequency Shift of the UV Detector with Different Light Power

Frequency shifts were also measured after the UV source is switched on for 10 seconds. Fig. 7 shows the response of a UV detector after 10 sec of UV Illumination with varying power density. The maximum detected frequency shifts are 19 kHz at 3.5mW/cm<sup>2</sup>, 10 kHz at 1.6mW/cm<sup>2</sup>, and 4 kHz at 0.5mW/cm<sup>2</sup>. Average frequency shifts of these measured data are 18 kHz, 9 kHz and 3 kHz corresponding to 3.5mW/cm<sup>2</sup>, 1.6mW/cm<sup>2</sup>, and 0.5mW/cm<sup>2</sup>. In the literature [19], maximum frequency shift of AlGaN-based SAW oscillator was less than 3 kHz at 1 to 2mW/cm<sup>2</sup> at 10 seconds after 365nm illumination. Therefore, the UV detector presented in this research has good sensitivity and fast response.

According to measurement results listed above, a UV detector utilizing the ZnO nanorod-based dual channel SAW oscillator system exhibited excellent sensitivity, reproducibility, and can exclude environmental fluctuations.

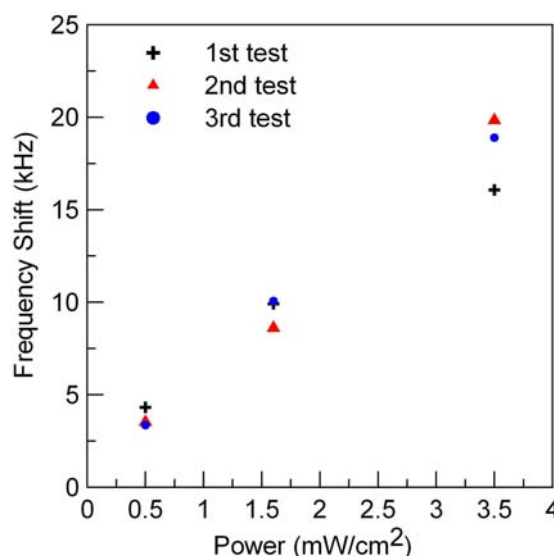


Fig.7 Frequency Shift of the Detector after 10 sec of UV Illumination

## 4 Conclusion

In this study, an ultraviolet detector based on a SAW oscillator system with ZnO-nanostructured sensing material is designed and realized. Responses of different light wavelengths and varied optical power are measured. Frequency shifts reach a maximum value of over 40 kHz at 365nm. Furthermore, frequency shifts is 19 kHz in 10 seconds after 365nm is on, much larger in comparison with the previously reported AlGaN/sapphire structure. These results show that performance of this UV detector such as sensitivity, response time, repeatability, and environmental-fluctuation elimination are excellent. In short, using ZnO nanorod as sensing material makes the SAW-based UV detector a promising candidate for UV sensing application.

## Acknowledgments

We are pleased to acknowledge Professor Chien-Ching Ma and Tsai-Ju Huang for their help with the instrument supplement of the UV source used in our measurements.

## References

- [1] M. H. Huang, Y. Wu, H. Feick, N. Tran, E. Weber, P. Yang, "Catalytic growth of zinc oxide nanowires by vapor transport", *Advanced Materials* 13, 113-116 (2001)
- [2] J. J. Wu, S. C. Liu, "Low-temperature growth of well-aligned ZnO nanorods by chemical vapor deposition", *Advanced Materials* 14, 215-218 (2002)
- [3] Z. W. Pan, Z. R. Dai, Z. L. Wang, "Nanobelts of semiconducting oxides", *Science* 291, 1947-1949 (2001)
- [4] M. H. Huang, S. Mao, H. Feick, H. Q. Yan, Y. Y. Wu, H. Kind, E. Weber, R. Russo, P. D. Yang, "Room-temperature ultraviolet nanowire nanolasers", *Science* 292, 1897-1899 (2002)
- [5] C. J. Park, D. K. Choi, J. Yoo, G. C. Yi, C. J. Lee, "Enhanced field emission properties from well-aligned zinc oxide nanoneedles grown on the Au/Ti/n-Si substrate", *Applied Physics Letters* 90, 083107 (2007)
- [6] M. Law, L. Greene, J. C. Johnson, R. Saykally, P. Yang, "Nanowire dye-sensitized solar cells", *Nature Materials* 4, 455-459 (2005)
- [7] Y. Zhang, K. Yu, D. Jiang, Z. Zhu, H. Geng, L. Luo, "Zinc oxide nanorod and nanowire for humidity sensor", *Applied Surface Science* 242, 212-217 (2005)
- [8] C. C. Li, Z. F. Du, L. M. Li, H. C. Yu, Q. Wan, T. H. Wang, "Surface-depletion controlled gas sensing of ZnO nanorods grown at room temperature", *Applied Physics Letters* 91, 032101 (2007)
- [9] A. Dorfman, N. Kumar, J. Hahm, "Highly sensitive biomolecular fluorescence detection using nanoscale ZnO platforms", *Langmuir* 22, 4890-4895 (2006)
- [10] A. Z. Sadek, W. Wlodarski, K. Shin, R. B. Kaner, K. Kalantar-Zadeh, "A layered surface acoustic wave gas sensor based on a polyaniline/In<sub>2</sub>O<sub>3</sub> nanofibre composite", *Nanotechnology* 17, 4488-4492 (2006)
- [11] T. T. Wu, Y. Y. Chen, T. H. Chou, "A high sensitivity nanomaterial based SAW humidity sensor", *Journal of Physics D: Applied Physics* 41, 085101 (2008)
- [12] A. Pohl, G. Ostermayer, L. Reindl, F. Seifert, "Monitoring the tire pressure at cars using passive SAW sensors", *Ultrasonics Symposium, 1997 Proceedings., 1997 IEEE* 1, 471-474 (1997)
- [13] T. M. A. Gronewold, A. Baumgartner, E. Quandt, M. Famulok, "Discrimination of single mutations in cancer-related gene fragments with a surface acoustic wave sensor", *Analytical Chemistry* 78, 4865-4871 (2006)
- [14] D. Ciplys, R. Rimeika, M. S. Shur, S. Rumyantsev, R. Gaska, A. Sereika, J. Yang, M. Asif Khan, "Visible-blind photoresponse of GaN-based surface acoustic wave oscillator", *Applied Physics Letters* 80, 2020-2022 (2002)
- [15] P. Sharma, K. Sreenivas, "Highly sensitive ultraviolet detector based on ZnO/LiNbO<sub>3</sub> hybrid surface acoustic wave filter", *Applied Physics Letters* 83, 3617-3619 (2003)
- [16] N. W. Emanetoglu, J. Zhu, Y. Chen, J. Zhong, Y. Chen, Y. Lu, "Surface acoustic wave ultraviolet photodetectors using epitaxial ZnO multilayers grown on r-plane sapphire", *Applied Physics Letters* 85, 3702-3704 (2004)
- [17] A. Wixforth, J. Scriba, M. Wassermeier, J. P. Kotthaus, G. Weimann, Q. Schlapp, "Surface acoustic waves on GaAs/Al<sub>x</sub>Ga<sub>1-x</sub>As heterostructures", *Physical Review B* 40, 7874-7887 (1989)
- [18] X. Feng, L. Feng, M. Jin, J. Zhai, L. Jiang, D. Zhu, "Reversible super-hydrophobicity to super hydrophilicity transition of aligned ZnO nanorod films", *Journal of the American Chemical Society* 126, 62-63 (2004)
- [19] D. Ciplys, M. S. Shur, N. Pala, A. Sereika, R. Rimeika, R. Gaska, Q. Fareed, "Ultraviolet-sensitive AlGaIn-based surface acoustic wave devices", *Sensors, 2004. Proceedings of IEEE* 3, 1345-1348 (2004)